Journal of Biomechanics 152 (2023) 111586

Contents lists available at ScienceDirect

Journal of Biomechanics

journal homepage: www.elsevier.com/locate/jbiomech

Exploration of muscle–tendon biomechanics one year after Achilles tendon rupture and the compensatory role of flexor hallucis longus

Ra'ad M. Khair [a,*], Lauri Stenroth [b], Neil J. Cronin [a,d], Ville Ponkilainen [c], Aleksi Reito [c], Taija Finni [a]

[a] Faculty of Sport and Health Sciences, Neuromuscular Research Center, University of Jyväskylä, Jyväskylä, Finland
[b] Department of Applied Physics, University of Eastern Finland, Kuopio, Finland
[c] Central Finland Central Hospital Nova, Jyväskylä, Finland
[d] School of Sport and Exercise, University of Gloucestershire, UK

ARTICLE INFO

Keywords:
Ultrasonography
Flexor hallucis longus muscle
Tendons
Function
Mechanical
Muscle

ABSTRACT

Achilles tendon (AT) rupture leads to long-term structural and functional impairments. Currently, the predictors of good recovery after rupture are poorly known. Thus, we aimed to explore the interconnections between structural, mechanical, and neuromuscular parameters and their associations with factors that could explain good recovery in patients with non-surgically treated AT rupture. A total of 35 patients with unilateral rupture (6 females) participated in this study. Muscle-tendon structural, mechanical, and neuromuscular parameters were measured 1-year after rupture. Interconnections between the inter-limb differences (Δ) were explored using partial correlations, followed by multivariable linear regression to find associations between the measured factors and the following markers that indicate good recovery: 1) tendon length, 2) tendon non-uniform displacement, and 3) flexor hallucis longus (FHL) normalized EMG amplitude difference between limbs. Δmedial gastrocnemius (MG) ($\beta = -0.12$, $p = 0.007$) and Δlateral gastrocnemius ($\beta = -0.086$, $p = 0.030$) subtendon lengths were associated with MG tendon Δstiffness. MG ($\beta = 11.56$, $p = 0.003$) and soleus ($\beta = 2.18$, $p = 0.040$) Δsubtendon lengths explained 48 % of variance in FHL EMG amplitude. Regression models for tendon length and non-uniform displacement were not significant. Smaller inter-limb differences in Achilles subtendon lengths were associated with smaller differences in the AT stiffness between limbs, and a smaller contribution of FHL muscle to the plantarflexion torque. In the injured limb, the increased contribution of FHL appears to partially counteract a smaller contribution from MG due to the elongated tendon, however the role of FHL should not be emphasized during rehabilitation to allow recovery of the TS muscles.

1. Introduction

Tendon rupture leads to long-term structural and mechanical changes in the Achilles tendon (AT) and the triceps surae (TS) muscles (Peng et al., 2019; Svensson et al., 2019). During the first 4 months after rupture, tendon length increases, and the extra length of the tendon alters the operating range of TS muscle sarcomeres, limiting their force generation ability due to the force–length relationship (Stäudle et al., 2020). The increase in tendon length has been found to be associated with inferior clinical and functional outcomes (Khair et al., 2022; Silbernagel et al., 2012a). Along with a change in tendon length, the TS muscles adapt by re-adjusting fascicle length and pennation angle, alleviating the loss of force production capability (Hullfish et al., 2019). Higher AT stiffness could also help to mitigate the impairments caused by tendon lengthening, preserving favourable sarcomere lengths during force generation by allowing the muscle to function within a smaller range (Stäudle et al., 2020).

The AT comprises distinct bundles of fascicles, called subtendons, that arise from the lateral (LG) and medial gastrocnemius (MG), and the soleus (SOL) muscles. Due to the different structure and force generating capacities of the TS muscles (Ward et al., 2009), AT is subjected to complex non-uniform loading that can cause heterogeneity of strain within the tendon (Bojsen-Møller and Magnusson, 2015). Recent in vivo studies have revealed that non-uniform motion within the AT is a function of a healthy tendon (Slane and Thelen, 2014), and might play an important role in the ability of the TS muscles to perform their

* Corresponding author.
E-mail address: raad.m.khair@jyu.fi (R.M. Khair).

https://doi.org/10.1016/j.jbiomech.2023.111586
Accepted 10 April 2023
Available online 13 April 2023

differing functional roles (Clark and Franz, 2021; Franz and Thelen, 2016). Ruptured AT displays more uniform mechanical behaviour after both surgical (Fröberg et al., 2017) and non-surgical treatment (Khair et al., 2021). Non-uniformity within the AT might be associated with TS fascicle length and the maximal amount that fascicles can shorten while exerting force. Thus, more uniform within-tendon displacement after rupture may stem from changes in TS structure and dynamics. Shortening of fascicles in the ruptured limb could result in a smaller operating range, translating to more uniform displacement within the AT. Understanding the associations between TS structural properties and within-AT displacement in patients with ATR could help to inform treatment and rehabilitation choices, leading to better functional outcomes.

Along with the well-documented structural and mechanical changes observed in the tendon after rupture, neuromuscular alterations also contribute to persistent performance deficits after ATR (Wenning et al., 2021). In the injured limb, increased TS muscle activity (Suydam et al., 2015; Wenning et al., 2021) and higher mean frequency of surface electromyography (EMG) (McHugh et al., 2019) have been reported previously in various tasks including eccentric and concentric contractions, indicating alterations in TS motor unit coordination and potentially a preferential activation of fast-twitch muscle fibers. Additionally, flexor hallucis longus (FHL) has been found to have a 5 % bigger cross-sectional area (CSA) in patients with ATR (Heikkinen et al., 2017). Motor control adapts to make greater use of FHL in plantarflexion due to altered force production capabilities in the TS muscles. This leads to a higher relative contribution of FHL to the plantarflexion torque produced in the ruptured limb, as observed in several studies of ATR patients (Finni et al., 2006; Heikkinen et al., 2017), and could be a potential marker of neuromuscular recovery.

Given the force and endurance deficits in plantarflexors after ATR (Khair et al., 2022; Silbernagel et al., 2012b), and the clinical importance of regaining capacity and functionality in the ruptured limb, it would be useful to understand the factors associated with markers of good recovery such as tendon lengthening after rupture, non-uniformity of internal tendon displacements, and neuromuscular alterations.

The aim of this study was to explore interconnections between structural, mechanical and neuromuscular parameters and their associations with markers of good recovery. Interconnections between factors were explored using partial correlations, followed by multivariable linear regression analysis to find associations between measured factors and the following markers of good recovery: 1) tendon length, 2) tendon non-uniform displacement, and 3) FHL normalized EMG amplitude difference between limbs. It was hypothesized that: 1) MG tendon stiffness would be associated with the lengthening of the tendon, 2) MG fascicle length and higher voluntary maximal plantarflexion torque would be related to non-uniformity within the AT, 3) EMG activity of the plantarflexors and the relative contribution of FHL during isometric contraction would be higher in the injured limb to counteract the structural deficits and be proportional to the increased length of the tendon after rupture.

2. Methods

We present data for thirty-five patients (6 females; means ± SD age: 41.1 ± 9.8 years, height: 175.9 ± 7.1 cm, mass: 83.1 ± 13.9 kg) with unilateral non-surgically treated ATR that participated voluntarily (NoARK, trial registration: NCT03704532). This study was approved by the Research Ethics Committee of Central Finland Health Care District (Approval number: 2U/2018). Participants were recruited through Central Finland Hospital (Nova) using the American Academy of Orthopaedic Surgeons guidelines. Inclusion criteria were a minimum of 2 of the following 4 criteria: a positive Thompson test, decreased plantarflexion strength, presence of a palpable gap, and increased passive ankle dorsiflexion with gentle manipulation (Reito et al., 2018). All participants were treated non-surgically with early mobilisation (Reito et al., 2018). Briefly, two weeks after full equinus cast, open cast was used to allow toe movement. At 4 weeks, weight bearing was encouraged with a custom-made special orthosis with 1 cm heel wedge. At week 8, the orthosis was removed and rehabilitation instructions were provided, however participants progressed individually and could consult a private physiotherapist if needed (Khair et al., 2022; Reito et al., 2018). Participants were tested (mean ± SD) 13 ± 1.7 months after rupture.

Upon arrival at the laboratory, both malleoli, heads of the fibula and first and fifth metatarsal heads were marked with a pen, and sagittal plane photos of the foot were taken from the medial and lateral side with a ruler beneath them as a reference to estimate the AT moment arm. AT thickness, TS subtendon length and MG fascicle length were measured from prone position with the foot relaxed over the edge of the bed. Achilles tendon resting angle (ATRA), MG and LG CSA were measured from the same position with the knee flexed to 90° and ankle in neutral position. All structural properties were measured using 3.6 and 6-cm linear probes (Aloka alpha10, Japan), and analysed using Image J. For detailed information on the collection and analysis please refer to (Khair et al., 2022).

For measurement of muscle activity, the skin was shaved and abraded with alcohol pads to reduce skin impedance. Disposable dual surface silver-silver electrode Ambu BlueSensor N electrodes (Ambu A/S, Ballerup, Denmark) were placed on the TS muscles with an interelectrode distance of 22 mm in accordance with SENIAM recommendations (Stegeman and Hermens, 2007). FHL electrodes were placed between the SOL insertion and the FHL muscle–tendon junction (MTJ) where only the FHL muscle belly lies (Péter et al., 2015), with an interelectrode distance of 16 mm. FHL electrode placement was confirmed during isolated big toe plantarflexion using ultrasound imaging. EMG signals were collected at 1500 Hz using a Noraxon wireless EMG system (Noraxon Inc., Scottsdale, AZ, USA). Data were not collected from five participants because of technical difficulties.

EMG data were filtered using a fourth order Butterworth filter between 20 and 450 Hz with a custom-made MATLAB script. Root mean square (RMS) envelopes were then computed using a moving 50 ms window and normalized to the RMS from a 1-*sec* window during MVC. The mean EMG amplitude of each muscle was calculated in a 1-*sec* window around the peak torque of the 30 % MVC contraction condition and used for further analysis. Total EMG activity of all plantarflexor muscles was also computed by summing SOL, MG, LG and FHL activity. This cumulative value denoted 100 % and was used to evaluate the relative contribution of each muscle to total plantarflexion activity (Masood et al., 2014).

After preparation, participants were seated in a custom-made ankle dynamometer (University of Jyväskylä, Finland) with hip, knee, ankle, and first metatarsophalangeal joints fixed at 120°, 0°, 90°, and 0° respectively. The seat was locked in position with the foot and thigh strapped to avoid any heel lift or postural changes during isometric contractions. A monitor was positioned in front of the participant to enable them to follow the torque signal in real time. After a series of submaximal contractions for warm-up, the participants performed unilateral maximal voluntary contractions (MVCs) starting with the non-injured limb. Participants tried to reach maximum torque in 2–3 s and decrease back to zero in 2–3 s, resulting in a 6-second pyramid-shaped torque curve. At least two MVCs were performed and the trial with the highest torque was used for further analysis. During the MVCs, MG-MTJ displacement was imaged at 70 Hz using the 6-cm linear probe.

Force data were collected via a transducer in the foot pedal of the ankle dynamometer, with a potentiometer placed under the heel to detect heel lift during contractions at 1 kHz. AT force was calculated using the individualized AT moment arm acquired from foot pictures. Tendon elongation and force recordings were synchronised to acquire AT force–length relations, and a second-order polynomial fit that was forced through the origin was calculated (Magnusson et al., 2001). For detailed information on the AT force and stiffness calculations please

refer to (Khair et al., 2022). In the text below, the term stiffness refers specifically to MG tendon stiffness.

After performing MVCs, participants were asked to perform ramp contractions corresponding to 30 % of the non-injured MVC, with the 3.6-cm linear probe attached longitudinally ~ 2 cm above the calcaneus to image displacement within the free tendon at 50 Hz. All data were sampled via a 16-bit A/D board (Power 1401, Cambridge Electronic Design, Cambridge, UK) connected to the lab computer, and signals were recorded using Spike2 software. To synchronize data, a TTL pulse was sent manually via Spike2 software (Cambridge Electronic Design, Cambridge, UK), which initiated the recording of the ultrasonography data for 8 s.

A 2D speckle tracking algorithm was used to evaluate AT tissue displacement from B-mode ultrasound videos according to the configuration of Slane and Thelen (Slane and Thelen, 2014). Briefly, superior-inferior displacements of six nodes across the width of the tendon were tracked and peak mean displacement was extracted (Slane and Thelen, 2014). Tendon non-uniformity was calculated as the difference between maximum and minimum displacement across the 6 locations. Lastly, displacement was normalized by dividing non-uniformity by the average peak displacement across all regions. Part of the AT displacement data used in this study was published previously in (Khair et al., 2021).

2.1. Statistical analysis

Statistical analysis was performed using JASP (JASP, Amsterdam, Netherlands). The descriptive data are reported as mean (SD). Pairwise T-tests were used to explore differences between limbs (injured vs non-injured) in structural, neuromechanical and mechanical properties after checking kurtosis and skewness of the data. Inter-limb differences (Δ) were calculated for all variables as percentage (%) difference between limbs: $\frac{Injured-non-njured}{non-injured}$*100 (Khair et al., 2022).

Partial correlations controlled for age and sex were performed to explore the interconnections between the measured biomechanical inter-limb differences. This was followed by multivariable linear regression to investigate variables associated with the following good recovery markers: 1) tendon length, 2) non-uniformity, and 3) FHL normalized EMG% amplitude. Covariates inclusion in models was based on previous knowledge (Clark and Franz, 2018; Hullfish et al., 2019; Stäudle et al., 2020), considering the associations detected in the exploratory correlations. For SOL subtendon model there was scarce previous literature concerning the length of the subtendon after rupture, so general variables that might influence free tendon length were included.

Considering the sample size, only four covariates were included in each model to avoid model overfitting. Age and sex were included in all models and complemented with two other variables. When investigating tendon length, the three AT subtendons had their own covariates: (a) MG model comprised of Δstiffness and ΔMG fascicle length, (b) LG model included Δstiffness and ΔLG CSA, and (c) the SOL model comprised of ΔATRA and Δstiffness. The non-uniformity model consisted of ΔMG fascicle length and ΔMVC. The FHL EMG% model was built with ΔMG subtendon length and ΔSOL subtendon length.

3. Results

Mean values and inter-limb differences are summarized in Table 1. For all measured variables except stiffness and LG-CSA, significant differences between limbs were detected. During submaximal isometric contraction at the same torque level, the combined cumulative RMS of the three TS muscles accounted for 81.9 % of the EMG activity in the non-injured limb compared to 75.8 % in the injured limb with no significant difference between limbs (Fig. 1). The relative MG contribution was lower in the injured limb with a mean difference of 0.061 (95 %CI 0.02–1.0). This was accompanied by an increased FHL contribution to total EMG in the injured limb, with a mean inter-limb difference of −0.061 (95 %CI −1.06 to −0.016).

Table 1
Descriptive data of measured variables and their inter-limb differences.

	Non-injured	Injured	Inter-limb difference (Δ)	p value
Measured at rest				
SOL subtendon length (cm)	8.79 ± 3.47	10.36 ± 3.71	29.1 %	p < 0.001*
MG subtendon length (cm)	18.90 ± 1.92	20.99 ± 2.20	11.4 %	p < 0.001*
LG subtendon length (cm)	21.59 ± 1.60	23.51 ± 1.99	9.1 %	p < 0.001*
AT thickness (cm)	0.48 ± 0.10	0.95 ± 0.22	99.8 %	p < 0.001*
ATRA°	129.34 ± 5.68	123.43 ± 6.88	−4.5 %	p < 0.001*
MG fascicle length (cm)	4.75 ± 0.76	3.75 ± 0.67	− 20.3 %	p < 0.001*
MG CSA (cm^2)	14.64 ± 3.91	12.59 ± 3.61	−13.5 %	p < 0.001*
LG CSA (cm^2)	7.79 ± 2.12	7.19 ± 2.74	−5.9 %	p = 0.091
Measured during MVC				
Stiffness (N/m)	639.23 ± 305.55	594.61 ± 337.51	−2.9 %	p = 0.328
MVC (Nm)	190.03 ± 65.76	158.94 ± 68.03	−19.7 %	p < 0.001*
Measured during 30 % of the non-injured MVC				
Non-uniformity (mm)	1.47 ± 1.02	0.91 ± 0.76	−11.6 %	p = 0.017*
Normalized non-uniformity	0.43 ± 0.29	0.26 ± 0.18	−11.4 %	p = 0.005*
SOL EMG (%)	21.4 ± 7.1	32.8 ± 17.8	67.3 %	p = 0.003*
MG EMG (%)	35.5 ± 11.9	45.0 ± 16.4	35.8 %	p < 0.001*
LG EMG (%)	22.4 ± 12.2	31.7 ± 20.7	65.5 %	p = 0.027*
FHL EMG (%)	19.5 ± 20.0	35.7 ± 21.4	176.3 %	p = 0.005*

Electromyography (EMG) activities are mean values of a 1-second window during the submaximal ramp contraction expressed as % of EMG recorded during maximal voluntary contraction. The submaximal plantarflexion torque level was the same in both limbs (30 % of the maximum of non-injured limbs). P-values refer to pair-wise T-test comparing the limbs with the asterisk indicating a significant difference between limbs ($p < 0.05$).

Inter-limb length differences of MG, SOL and LG subtendons were positively associated with higher ΔFHL normalized EMG% amplitude. Stiffness inter-limb difference was negatively correlated with MG and LG Δsubtendon lengths. All other associations between structural and neuromuscular inter-limb differences are presented in Fig. 2.

The MG subtendon length model explained 26 % of the variance ($F(4,27) = 2.63$, $p = 0.056$) with RMSE of 9.06. ΔStiffness was associated with ΔMG subtendon length ($\beta = -0.12$, [95 %CI −0.20 to −0.03]). In the LG subtendon model, where 19 % of the variance was explained ($F(4,26) = 1.52$, $p = 0.225$) with RMSE of 8.26, Δstiffness was associated with ΔLG subtendon length ($\beta = -0.086$, [95 %CI −0.16 to −0.006]). SOL subtendon length model explained 20 % of the variance ($F(4,31) = 1.72$, $p = 0.174$) with RMSE of 37.09. There were no detectable associations between ΔATRA ($\beta = 0.38$, [95 %CI −2.14 to 2.91]), or Δstiffness ($\beta = 0.05$, [95 %CI −0.30 to 0.40]) and ΔSOL subtendon length.

The non-uniformity model explained 11 % of the variance ($F(4,30) = 0.96$, $p = 0.44$) with RMSE of 149.58. ΔMG fascicle length ($\beta = 5.08$, [95 %CI −0.64 to 10.80]) and ΔMVC ($\beta = -2.49$, [95 %CI −6.36 to 1.40]) were not associated with the inter-limb difference in AT non-uniformity.

The FHL normalized EMG% amplitude model explained 48 % of the variance ($F(5,21) = 3.83$, $p = 0.0127$) with RMSE of 150.5. MG (β =

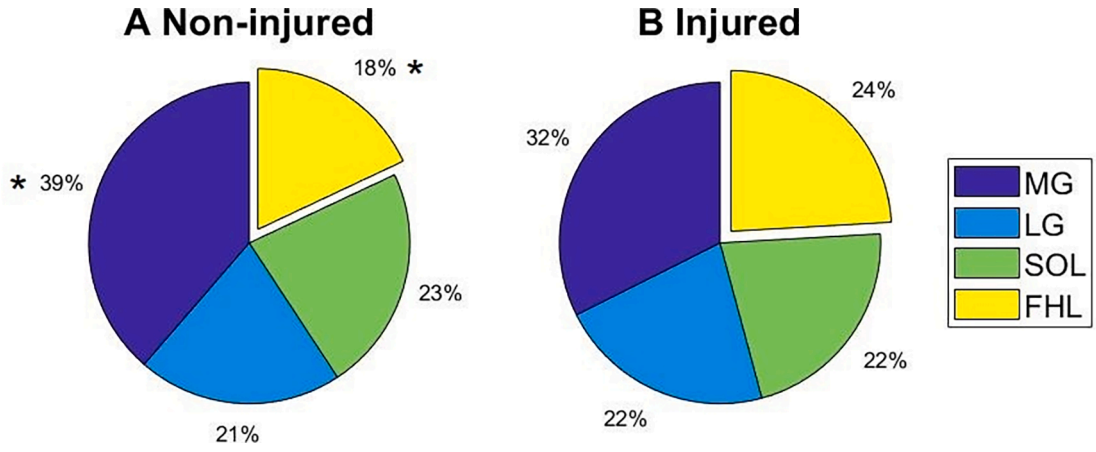

Fig. 1. Relative contribution of medial gastrocnemius (MG), lateral gastrocnemius (LG), soleus (SOL) and flexor hallucis longus (FHL) to total cumulative EMG activity during submaximal ramp isometric contraction in the non-injured (A) and injured limbs (B). * Significant difference between limbs within a given muscle ($p < 0.05$).

11.56, [95 %CI 4.22–18.90]) and SOL Δsubtendon lengths (β = 2.18, [95 %CI 0.10–4.05]) were both significantly associated with FHL ΔEMG activity.

4. Discussion

The main finding was the higher relative contribution of FHL to the summed normalized EMG activity in the injured compared to the non-injured limb at the same submaximal isometric torque level. The greater relative FHL activity was of similar magnitude to the decrease in MG activity, suggesting a crucial role of FHL in compensating for the reduced force production capacity after ATR. Additionally, differences in tendon length were associated with greater FHL mean amplitude difference between limbs; the more elongated the injured tendon, the greater the relative FHL activity. Lastly, lengthening of the gastrocnemii muscle subtendons after rupture was negatively associated with the difference in stiffness between limbs.

The mean EMG amplitudes of all TS muscles were higher in the injured limb during submaximal isometric contractions. This could be a result of the TS muscle functioning outside the optimum region on the force–length curve, where greater activity is needed to achieve the same absolute torque as the contralateral limb (Suydam et al., 2015). McHugh and colleagues found an increased median frequency of TS EMG in patients with plantarflexion weakness after ATR, and this was more pronounced in patients with excessive tendon lengthening (McHugh et al., 2019). It should be noted that the testing was done in neutral ankle position. Strength deficits after ATR manifest especially when the ankle is in the end-range of plantar flexion. Mullaney and colleagues found an average of 27 % plantar flexion strength deficits when the ankle was in a plantar flexed position but did not observe weakness when the ankle was in dorsi flexion (Mullaney et al., 2006). Thus, it may be that the current sample would show larger neuromuscular and strength impairments in plantar flexed ankle position.

In addition to potential changes in the sarcomere level operating length of the TS muscles, decreased muscle physiological CSA necessitates increased muscle activity to reach a given joint moment in the injured limb. It should be noted that, in accordance with previous studies (Aufwerber et al., 2020; Nicholson et al., 2020), LG was less atrophied and did not demonstrate the same magnitude of difference in CSA as seen in MG, but higher EMG activity was still observed in LG.

In our sample, SOL subtendon length was on average 1.56 cm longer in the injured limb, and although this was less than observed in the gastrocnemii, it resulted in an almost 30 % longer SOL subtendon than on the contralateral side. Furthermore, SOL showed the highest difference in EMG activity among the TS muscles compared to the contralateral limb, suggesting that SOL structure and force production capacity were affected the most by tendon lengthening.

The relative contribution of FHL was 8 % higher in the injured limb, whereas in MG the contribution was 7 % lower compared to the non-injured limb. Compensatory strategies likely start shortly after rupture, where force is averted away from the freshly ruptured AT by increasing the contribution of FHL to plantarflexion torque. This motor strategy may become a persistent feature in ATR patients. Altered motor control may be driven by the potentially disadvantageous position of the TS muscles on the force–length curve. The shift in the TS operating range on the force–length curve (Suydam et al., 2015), and changes in the TS muscles, corresponds to the degree of increase in tendon length after rupture, which seems to be the primary cause of structural and neuromechanical changes. Indeed, we found that patients whose FHL EMG% activity was higher in the injured limb also exhibited greater inter-limb differences in tendon length. It is true that TS muscle weakness is partially compensated by FHL but FHL capacity to compensate for the loss of strength in the injured limb is limited due to relatively short plantarflexion moment arm. Thus, treatments and rehabilitation should not emphasize the role of FHL to allow recovery of the TS, and aim to minimize tendon lengthening after ATR.

As we have shown previously (Khair et al., 2021), our sample showed more uniform displacement within the injured tendon at the same absolute torque, even when non-uniformity was normalized, indicating that mechanical sliding within the tendon fascicles was impaired after ATR. A more uniform displacement within the tendon might limit the ability of the TS muscle to perform their different functional roles in the most optimal way (Clark and Franz, 2021; Franz and Thelen, 2016). Contrary to our initial idea that MG and SOL muscle activity may mirror the differences in non-uniformity (Clark and Franz, 2018), we did not find such associations. However, shorter fascicles likely result in a shorter operating range and quick saturation of TS force production (De la Fuente et al., 2016; Khair et al., 2022), reducing displacement and non-uniformity within the tendon.

Stiffness was negatively associated with the increased length of both gastrocnemii muscle subtendons in agreement with our previous study, where we found that stiffness was associated with MG subtendon length inter-limb difference (Khair et al., 2022). However, in the present study, the interlimb difference in SOL subtendon length was not associated with the stiffness difference between limbs. This is primarily because stiffness was calculated from displacement at the MG-MTJ, and locally the stiffness values might differ at the SOL insertion. Lengthening of the tendon after rupture would result in lower stiffness. For example, if we compare two tendons with the same mechanical properties, a longer tendon would elongate more under the same load, and the change in the

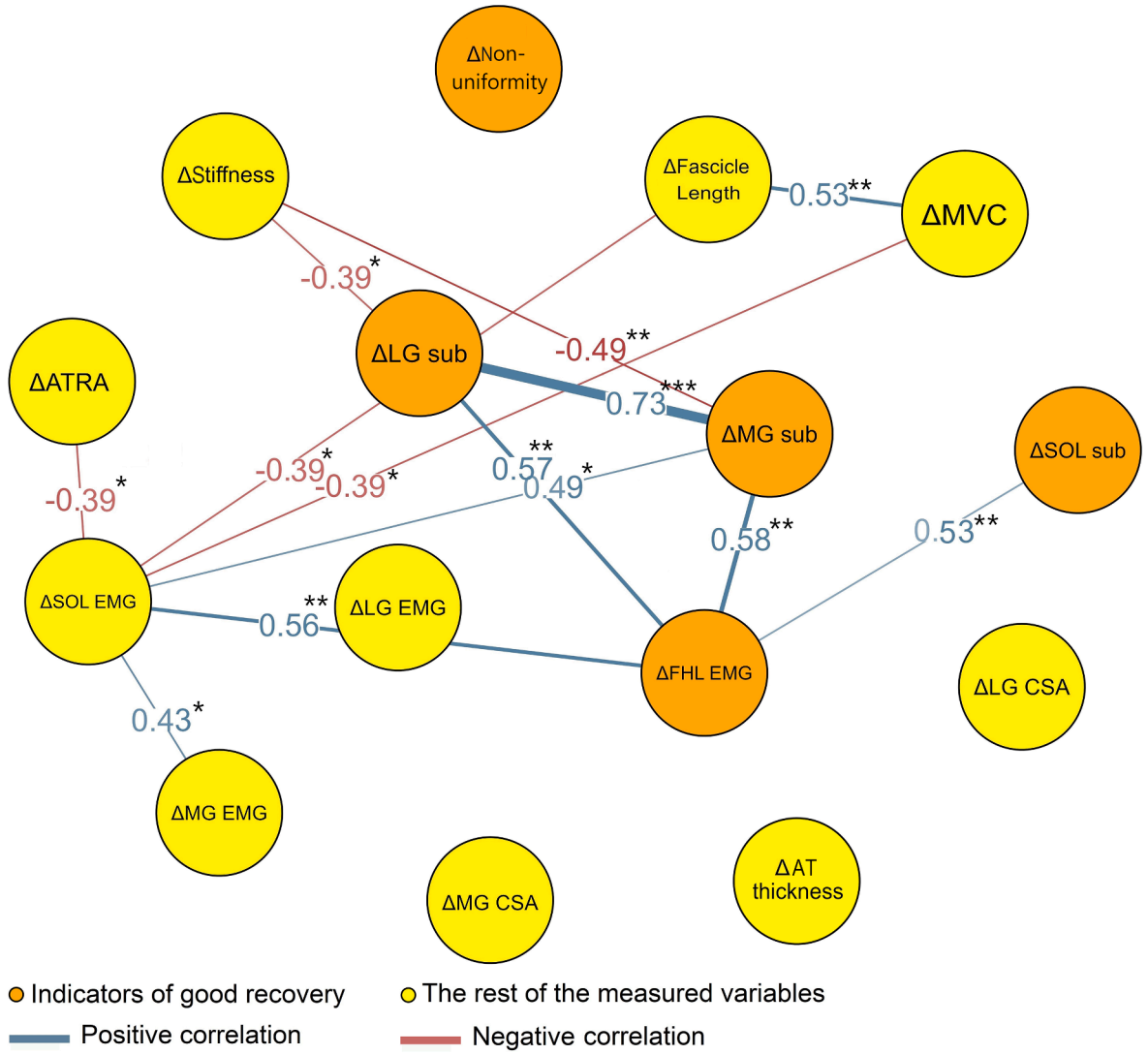

Fig. 2. Network plot exploring the connections between interlimb (Δ) differences in structural and neuromechanical variables. The nodes are positioned using Fruchterman-Reingold algorithm which organizes the network based on the strength of the connections between nodes (Epskamp et al., 2012). Edges between nodes indicate significant interactions with the correlation coefficient outlined on the edge between any two nodes. Blue edges indicate a positive correlation, and red indicates a negative correlation. Orange nodes represent factors that we chose to explore as indicators of good recovery, and yellow nodes represent the other measured variables. *$p < 0.05$, **$p < 0.01$, ***$p < 0.001$. (For interpretation of the references to colour in this figure legend, the reader is referred to the web version of this article.)

force–elongation slope would be directly proportional to the extra length of the tendon (Proske and Morgan, 1987). Considering the previously observed association between muscle strength and tendon stiffness (Arampatzis et al., 2007), it can be speculated that improving muscle strength could help to ameliorate, albeit not completely prevent, the adverse effects of tendon lengthening in patients with ATR. In the early rehabilitation phase, there is a potential risk of excessive tendon lengthening if the tendon is overloaded. Rehabilitative measures, such as blood flow restriction which have been shown to increase tendon stiffness with low mechanical loading (Centner et al., 2019), may be beneficial to induce necessary stimulus especially in the early phase of recovery where loss of muscle strength my prevent proper loading of the tendon.

4.1. Limitations

As commonly recommended, EMG values were normalized to RMS during MVCs. This method may be prone to errors, including the possibility that the ankle flexors were not fully activated during maximal contractions. Thus, caution should be taken when making inferences based on the findings. However, this does not invalidate our results showing that motor control of ankle plantarflexors during submaximal effort differs between limbs in ATR patients, which is consistent with previous studies (McHugh et al., 2019; Wenning et al., 2021).

5. Conclusion

Relative FHL muscle activity was higher in the injured compared to the non-injured limb during submaximal plantarflexion, and this appeared to compensate for decreased MG activity. Despite higher EMG activity in all muscles, plantarflexion maximum torque was still lower in the injured limb. Excessive lengthening of the tendon after ATR is associated with lower stiffness, worsening the ramifications of the rupture.

CRediT authorship contribution statement

Ra'ad M. Khair: Writing – original draft, Writing – review & editing,

Data curation, Visualization, Investigation, Formal analysis, Conceptualization. **Lauri Stenroth:** Methodology, Conceptualization, Writing – review & editing. **Neil J. Cronin:** Supervision, Methodology, Conceptualization, Writing – review & editing. **Ville Ponkilainen:** Writing – review & editing. **Aleksi Reito:** Writing – review & editing, Methodology, Conceptualization. **Taija Finni:** Writing – review & editing, Supervision, Resources, Project administration, Methodology, Funding acquisition, Conceptualization.

Declaration of Competing Interest

The authors declare that they have no known competing financial interests or personal relationships that could have appeared to influence the work reported in this paper.

Data availability

Data used in this manuscript is available for viewing with reasonable request.

Acknowledgments

This work was supported by Academy of Finland (grant #323168), UNderstanding RESToration of Achilles Tendon function after rupture (UNRESAT). The funding organization had no role in collection, analysis and interpretation of the data, or publication.

References

Arampatzis, A., Karamanidis, K., Morey-Klapsing, G., De Monte, G., Stafilidis, S., 2007. Mechanical properties of the triceps surae tendon and aponeurosis in relation to intensity of sport activity. J. Biomech. 40, 1946–1952. https://doi.org/10.1016/j.jbiomech.2006.09.005.

Aufwerber, S., Edman, G., Grävare Silbernagel, K., Ackermann, P.W., 2020. Changes in tendon elongation and muscle atrophy over time after Achilles tendon rupture repair: a prospective cohort study on the effects of early functional mobilization. Am. J. Sports Med. 48, 3296–3305. https://doi.org/10.1177/0363546520956677.

Bojsen-Møller, J., Magnusson, S.P., 2015. Heterogeneous loading of the human Achilles tendon in vivo. Exerc. Sport Sci. Rev. 43, 190–197. https://doi.org/10.1249/JES.0000000000000062.

Centner, C., Lauber, B., Seynnes, O.R., Jerger, S., Sohnius, T., Gollhofer, A., König, D., 2019. Low-load blood flow restriction training induces similar morphological and mechanical Achilles tendon adaptations compared with high-load resistance training. J. Appl. Physiol. 127, 1660–1667. https://doi.org/10.1152/japplphysiol.00602.2019.

Clark, W.H., Franz, J.R., 2018. Do triceps surae muscle dynamics govern non-uniform Achilles tendon deformations? PeerJ 6, e5182.

Clark, W.H., Franz, J.R., 2021. Age-related changes to triceps surae muscle-subtendon interaction dynamics during walking. Sci. Rep. 11, 21264. https://doi.org/10.1038/s41598-021-00451-y.

De la Fuente, C.I., Lillo, R.P., Ramirez-Campillo, R., Ortega-Auriol, P., Delgado, M., Alvarez-Ruf, J., Carreño, G., 2016. Medial gastrocnemius myotendinous junction displacement and plantar-flexion strength in patients treated with immediate rehabilitation after Achilles tendon repair. J. Athl. Train. 51, 1013–1021.

Epskamp, S., Cramer, A.O.J., Waldorp, L.J., Schmittmann, V.D., Borsboom, D., 2012. qgraph: Network visualizations of relationships in psychometric data. J. Stat. Softw. 48, 1–18. https://doi.org/10.18637/jss.v048.i04.

Finni, T., Hodgson, J.A., Lai, A.M., Edgerton, V.R., Sinha, S., 2006. Muscle synergism during isometric plantarflexion in Achilles tendon rupture patients and in normal subjects revealed by velocity-encoded cine phase-contrast MRI. Clin. Biomech. 21, 67–74.

Franz, J.R., Thelen, D.G., 2016. Imaging and simulation of Achilles tendon dynamics: implications for walking performance in the elderly. J. Biomech. 49, 1403–1410. https://doi.org/10.1016/j.jbiomech.2016.04.032.

Fröberg, Å., Cissé, A.-S., Larsson, M., Mårtensson, M., Peolsson, M., Movin, T., Arndt, A., 2017. Altered patterns of displacement within the Achilles tendon following surgical repair. Knee Surg. Sports Traumatol. Arthrosc. 25, 1857–1865.

Heikkinen, J., Lantto, I., Piilonen, J., Flinkkilä, T., Ohtonen, P., Siira, P., Laine, V., Niinimäki, J., Pajala, A., Leppilahti, J., 2017. Tendon length, calf muscle atrophy, and strength deficit after acute Achilles tendon rupture: long-term follow-up of patients in a previous study. JBJS 99, 1509–1515.

Hullfish, T.J., O'Connor, K.M., Baxter, J.R., 2019. Medial gastrocnemius muscle remodeling correlates with reduced plantarflexor kinetics 14 weeks following Achilles tendon rupture. J. Appl. Physiol. Bethesda Md 1985 (127), 1005–1011. https://doi.org/10.1152/japplphysiol.00255.2019.

Khair, R.M., Stenroth, L., Péter, A., Cronin, N.J., Reito, A., Paloneva, J., Finni, T., 2021. Non-uniform displacement within ruptured Achilles tendon during isometric contraction. Scand. J. Med. Sci. Sports 31, 1069–1077. https://doi.org/10.1111/sms.13925.

Khair, R.M., Stenroth, L., Cronin, N.J., Reito, A., Paloneva, J., Finni, T., 2022. Muscle-tendon morphomechanical properties of non-surgically treated Achilles tendon 1-year post-rupture. Clin. Biomech. 92, 105568 https://doi.org/10.1016/j.clinbiomech.2021.105568.

Magnusson, S.P., Aagaard, P., Rosager, S., Dyhre-Poulsen, P., Kjaer, M., 2001. Load-displacement properties of the human triceps surae aponeurosis in vivo. J. Physiol. 531, 277–288. https://doi.org/10.1111/j.1469-7793.2001.0277j.x.

Masood, T., Bojsen-Møller, J., Kalliokoski, K.K., Kirjavainen, A., Äärimaa, V., Peter Magnusson, S., Finni, T., 2014. Differential contributions of ankle plantarflexors during submaximal isometric muscle action: A PET and EMG study. J. Electromyogr. Kinesiol. 24, 367–374. https://doi.org/10.1016/j.jelekin.2014.03.002.

McHugh, M.P., Orishimo, K.F., Kremenic, I.J., Adelman, J., Nicholas, S.J., 2019. Electromyographic evidence of excessive Achilles tendon elongation during isometric contractions after Achilles tendon repair. Orthop. J. Sports Med. 7, 2325967119883357 https://doi.org/10.1177/2325967119883357.

Mullaney, M.J., McHugh, M.P., Tyler, T.F., Nicholas, S.J., Lee, S.J., 2006. Weakness in end-range plantar flexion after Achilles tendon repair. Am. J. Sports Med. 34, 1120–1125. https://doi.org/10.1177/0363546505284186.

Nicholson, G., Walker, J., Dawson, Z., Bissas, A., Harris, N., 2020. Morphological and functional outcomes of operatively treated Achilles tendon ruptures. Phys. Sportsmed. 48, 290–297. https://doi.org/10.1080/00913847.2019.1685364.

Peng, W.C., Chao, Y.H., Fu, A.S.N., Fong, S.S.M., Rolf, C., Chiang, H., Chen, S., Wang, H. K., 2019. Muscular morphomechanical characteristics after an Achilles repair. Foot Ankle Int. 40, 568–577. https://doi.org/10.1177/1071100718822537.

Péter, A., Hegyi, A., Stenroth, L., Finni, T., Cronin, N.J., 2015. EMG and force production of the flexor hallucis longus muscle in isometric plantarflexion and the push-off phase of walking. J. Biomech. 48, 3413–3419. https://doi.org/10.1016/j.jbiomech.2015.05.033.

Proske, U., Morgan, D.L., 1987. Tendon stiffness: methods of measurement and significance for the control of movement: a review. J. Biomech. 20, 75–82. https://doi.org/10.1016/0021-9290(87)90269-7.

Reito, A., Logren, H.-L., Ahonen, K., Nurmi, H., Paloneva, J., 2018. Risk factors for failed nonoperative treatment and rerupture in acute Achilles tendon rupture. Foot Ankle Int. 39, 694–703.

Silbernagel, K.G., Steele, R., Manal, K., 2012. Deficits in heel-rise height and Achilles tendon elongation occur in patients recovering from an Achilles tendon rupture. Am. J. Sports Med. 40, 1564–1571. https://doi.org/10.1177/0363546512447926.

Slane, L.C., Thelen, D.G., 2014. The use of 2D ultrasound elastography for measuring tendon motion and strain. J. Biomech. 47, 750–754.

Stäudle, B., Seynnes, O., Laps, G., Göll, F., Brüggemann, G.-P., Albracht, K., 2020. Recovery from Achilles tendon repair: a combination of postsurgery outcomes and insufficient remodeling of muscle and tendon. Med. Sci. Sports Exerc. Publish Ahead of Print. https://doi.org/10.1249/MSS.0000000000002592.

Stegeman, D., Hermens, H., 2007. Standards for surface electromyography: the European project Surface EMG for non-invasive assessment of muscles (SENIAM). Enschede Roessingh Res. Dev. 10, 8–12.

Suydam, S.M., Buchanan, T.S., Manal, K., Silbernagel, K.G., 2015. Compensatory muscle activation caused by tendon lengthening post-Achilles tendon rupture. Knee Surg. Sports Traumatol. Arthrosc. 23, 868–874. https://doi.org/10.1007/s00167-013-2512-1.

Svensson, R.B., Couppé, C., Agergaard, A.-S., Ohrhammar Josefsen, C., Jensen, M.H., Barfod, K.W., Nybing, J.D., Hansen, P., Krogsgaard, M., Magnusson, S.P., 2019. Persistent functional loss following ruptured Achilles tendon is associated with reduced gastrocnemius muscle fascicle length, elongated gastrocnemius and soleus tendon, and reduced muscle cross-sectional area. Transl. SPORTS Med. 2, 316–324. https://doi.org/10.1002/tsm2.103.

Ward, S.R., Eng, C.M., Smallwood, L.H., Lieber, R.L., 2009. Are current measurements of lower extremity muscle architecture accurate? Clin. Orthop. 467, 1074–1082. https://doi.org/10.1007/s11999-008-0594-8.

Wenning, M., Mauch, M., Heitner, A., Lienhard, J., Ritzmann, R., Paul, J., 2021. Neuromechanical activation of triceps surae muscle remains altered at 3.5 years following open surgical repair of acute Achilles tendon rupture. Knee Surg. Sports Traumatol. Arthrosc. 29, 2517–2527. https://doi.org/10.1007/s00167-021-06512-z.